A machine learning algorithm for detecting abnormal respiratory cycles in thoracic dynamic MR image acquisitions

Changjian Sun, Jayaram K. Udupa, Yubing Tong, Caiyun Wu, Shuxu Guo, et al.

Changjian Sun, Jayaram K. Udupa, Yubing Tong, Caiyun Wu, Shuxu Guo, Drew A. Torigian, Robert M. Campbell Jr., "A machine learning algorithm for detecting abnormal respiratory cycles in thoracic dynamic MR image acquisitions," Proc. SPIE 10948, Medical Imaging 2019: Physics of Medical Imaging, 109484E (1 March 2019); doi: 10.1117/12.2513453

SPIE.

Event: SPIE Medical Imaging, 2019, San Diego, California, United States

A machine learning algorithm for detecting abnormal respiratory cycles in thoracic dynamic MR image acquisitions

Changjian Sun[1, 2], Jayaram K. Udupa[2*], Yubing Tong[2], Caiyun Wu[2], Shuxu Guo[1], Drew A. Torigian[2], Robert M. Campbell[3]

[1.] College of Electronic Science and Engineering, Jilin University, Changchun, China.

[2.] Medical Image Processing Group, 602 Goddard building, 3710 Hamilton Walk, Department of Radiology, University of Pennsylvania, Philadelphia, PA 19104, United States.

[3.] Center for Thoracic Insufficiency Syndrome, Children's Hospital of Philadelphia, Philadelphia, PA, 19104, United States

ABSTRACT

4D image construction of thoracic dynamic MRI data provides clinicians the capability of examining the dynamic function of the left and right lungs, left and right diaphragms, and left and right chest wall separately. For the method implemented based on free-breathing rapid 2D slice acquisitions, often part of the acquired data cannot be used for the 4D image reconstruction algorithm because some patients hold their breath or breathe in patterns that differ from regular tidal breathing. Manually eliminating abnormal image slices representing such abnormal breathing is very labor intensive considering that typical acquisitions contain ~3000 slices. This paper presents a novel respiratory signal classification algorithm based on optical flow techniques and a SVM classifier. The optical flow technique is used to track the speed of the diaphragm, and the motion features are extracted to train the SVM classification model. Due to the limited number of abnormal samples usually observed, 118 abnormal signals were generated by simulation by appropriately transforming the normal signals, so that the number of normal and abnormal signals reached 160 and 160, respectively. In the process of model training, our goal is to reduce the error rate of false negative abnormal signal detection (FN) as much as possible even at the cost of increasing false positive misclassification rate (FP) for normal signals. From 10 experiments we conducted, the average FN rate and FP rate reached 5% and 26%, respectively. The accuracy over all (real and simulated) samples was 85%. In all real samples, 82% of the abnormal data were correctly detected.

1. INTRODUCTION

4D image construction and analysis of the thorax based on thoracic dynamic magnetic resonance imaging (dMRI) acquisitions provides critical information about lung function. These techniques facilitate studying lung function separately for left and right lungs, left and right hemi-diaphragms, and left and right chest wall components, which is also useful to assess thoracic insufficiency syndrome (TIS) and its surgical treatment [1, 2, 3]. In most cases, children with TIS are born with congenital spinal disorders, such as scoliosis, and often malformed ribs [2, 3]. Severe TIS patients are unable to support normal breathing and lung growth. As they grow, lung size and proper respiratory motion are limited and such patients may become dependent on nasal oxygen or ventilator support to breathe.

Traditional 4D imaging methods are difficult to implement for studying TIS patients due to the pathophysiological characteristics of these patients. For example, patients often suffer from extreme deformities of the chest wall, diaphragm, and/or spine that prevent the chest from supporting normal breathing to cooperate with the requirements of imaging such as breath-holding or breathing cooperatively with a gating or tracking device [2, 3]. Therefore, for the study of TIS, image acquisition under free-breathing conditions is the only practical option. With this tenet, we developed a method of dMRI,

Medical Imaging 2019: Physics of Medical Imaging, edited by Taly Gilat Schmidt, Guang-Hong Chen, Hilde Bosmans,
Proc. of SPIE Vol. 10948, 109484E · © 2019 SPIE · CCC code: 1605-7422/19/$18 · doi: 10.1117/12.2513453

wherein for each sagittal slice location through the thorax, slices are acquired over several respiratory cycles at ~200 ms per slice while the patient breathes freely. Images are acquired in this manner for all sagittal locations across the chest. This typically results in ~3000 slices in one dMRI acquisition which constitute a spatio-temporal sampling of the dynamic thorax. From these data, by using a graph-based optimization technique [1], we construct an "optimal" 4D image representing the breathing thorax over one respiratory cycle, which typically consists of ~300 spatio-temporal slices. The method is purely-image based without the requirement of sorting based on a breathing signal or using any external surrogates.

During the data acquisition process, although the patients are instructed to breath normally and uniformly, often they hold their breath momentarily, take very shallow or deep breaths, or breathe irregularly compared to what may be characterized as regular tidal breathing. This corrupts the acquired data and may mislead the 4D construction method and the dynamics derived from the 4D image. Since the number of acquired 2D slices is ~3000, the cost of manually identifying and eliminating such cycles and slices is very high. This paper presents a machine learning method to automatically identify such abnormal breathing cycles in the time sequence of acquired slices for each sagittal location.

2. MATERIALS AND METHODS

Image data

Experiments are carried out on image data from the Children's Hospital of Philadelphia (CHOP). This retrospective study was conducted following approval from the Institutional Review Board at CHOP along with a Health Insurance Portability and Accountability Act waiver. Thoracic dMRI data utilized in this paper include, for each of 30-40 sagittal slice locations across the chest, 80 time slices acquired continuously under tidal breathing conditions at a rate of ~200 ms per slice. The slices are 224×256 pixels with a pixel size of 1.47×1.47 mm. Subjects included were 11 TIS patients with various malformations of the rib cage and/or spine, where 5 patients provided normal breathing pattern data and 6 patients had abnormal breathing patterns. From the perspective of detecting abnormal respiratory cycles, our data consisted of a total of ~380 sagittal locations (or time sequences) out of which 42 sagittal locations from data from 6 patients contained abnormal cycles and the remaining 338 contained normal cycles.

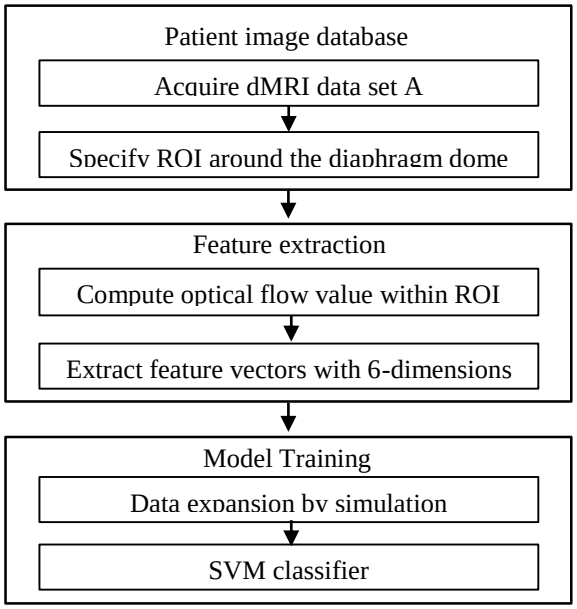

Figure 1. Flow chart of detecting abnormal respiratory cycles.

Main idea of auto-labeling

The main idea of the method is to train a classifier for respiratory signal discrimination. Each time-series of slices of the patient's breathing pattern corresponding to a sagittal slice location is used to generate signals representing breathing cycles in the series, and the features of the extracted signals are trained using a machine learning method to obtain a classification model that can weed out the abnormal respiratory cycles in the sequence as accurately as possible. Firstly, we use the diaphragm indicated within a region of interest (ROI) as a surrogate to track upward and downward motion of the thorax during the inspiration and expiration phases of the respiratory cycle. Then, an optical flow approach [4] is employed to automatically track the motion of the hemi-diaphragm at each sagittal slice location. Features are designed to distinguish between normal and abnormal respiratory signals. Finally, we train an SVM-based [5] model to detect abnormal signals and follow the strategy of reducing FN as much as possible to detect abnormal signals. An overview of the detection approach is schematically illustrated in Figure 1.

Feature construction of respiratory signals

Manually discriminating between normal and abnormal breathing patterns is based on observing the movement of the diaphragm in the time series of 80 time slices for each sagittal location [6]. During normal breathing, the diaphragm moves approximately uniformly over all 80 time points. When a patient holds his/her breath or takes very shallow breaths, the diaphragm may be near static for several consecutive time points at this scanning position. Therefore, compared with normal breathing, the diaphragm movement in abnormal breathing is significantly lower during such respiratory periods. This means that there is a significant reduction in the speed of motion of the diaphragm. Similarly, when a patient takes very deep breaths, the diaphragm may move significantly faster than during regular tidal breathing. Lastly, when a patient breathes irregularly, the diaphragm may move significantly slower or faster at different time points during the respiratory cycle.

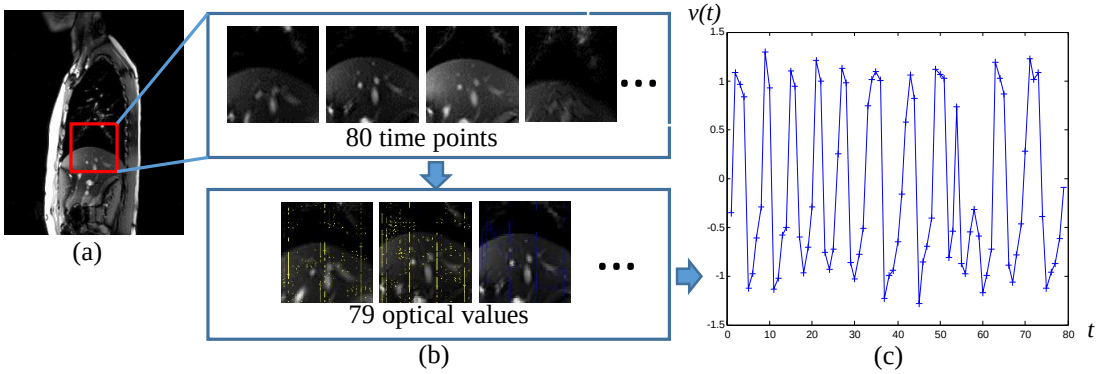

Figure 2. (a) An ROI covering the diaphragm dome. (b) Flow values from 4 adjoining time slices. Yellow arrows indicate positive values and blue arrows indicate negative values. (c) The horizontal axis corresponds to time point t and the vertical axis denotes magnitude of velocity or signed speed $v(t)$.

Optical flow is an image analysis technique which can estimate the speed of pixel movement from a time series of images by examining adjacent time slices in the series. This technique can be employed to track the diaphragm speed from every pair of adjacent time slices. The flow value is a vector that contains speed and direction information. A region of interest (ROI) containing the part of the diaphragm is selected for estimating the optical flow matrix at every pixel within the ROI from adjacent time point slices. The mean of the optical flow vectors associated with all pixels within the ROI is taken to approximate the velocity of the diaphragm between adjacent time slices. For each sagittal position, 79 velocities are obtained over 80 time points by considering the current and next time point in this manner. During the inhalation process, the diaphragm moves downward and the direction of flow is considered to be positive, and during exhalation, this phenomenon is reversed where the diaphragm moves upward and the direction of flow is considered negative. We will denote the signed magnitude of velocity (or signed speed) by $v(t)$. During normal breathing, the maximum speed of the diaphragm estimated at the 79 time points (or respiratory phases) remains roughly the same. However, when a patient

alters his/her regular breathing, the speed may be much lower or higher compared to that in normal breathing, which is reflected in the flow values of the ROI. Figure 2 shows the process of tracking diaphragm motion through optical flow.

The difference in velocity values $v(t)$ between normal breathing and abnormal breathing can be used to screen out abnormal breathing signals. Figure 3 displays the $v(t)$ curves of normal and abnormal breathing. For example, when a patient does shallow breathing, the $v(t)$ signal fluctuates in a small range, as demonstrated in Figure 3 b(1) for an actual patient signal. During this phase, the local extrema of the $v(t)$ values (Figure 3 b(2)) at some time points (e.g., at 0-5) are much lower than similar entities in normal respiration as illustrated in Figure 3 a(2). Exploiting this characteristic, we take the local extrema of all respiratory cycles, separate out all positive and negative values, select the maximum, minimum, and median values for all positive and negative values separately, and use them as features. Thus, the feature vector is a 6-dimensional

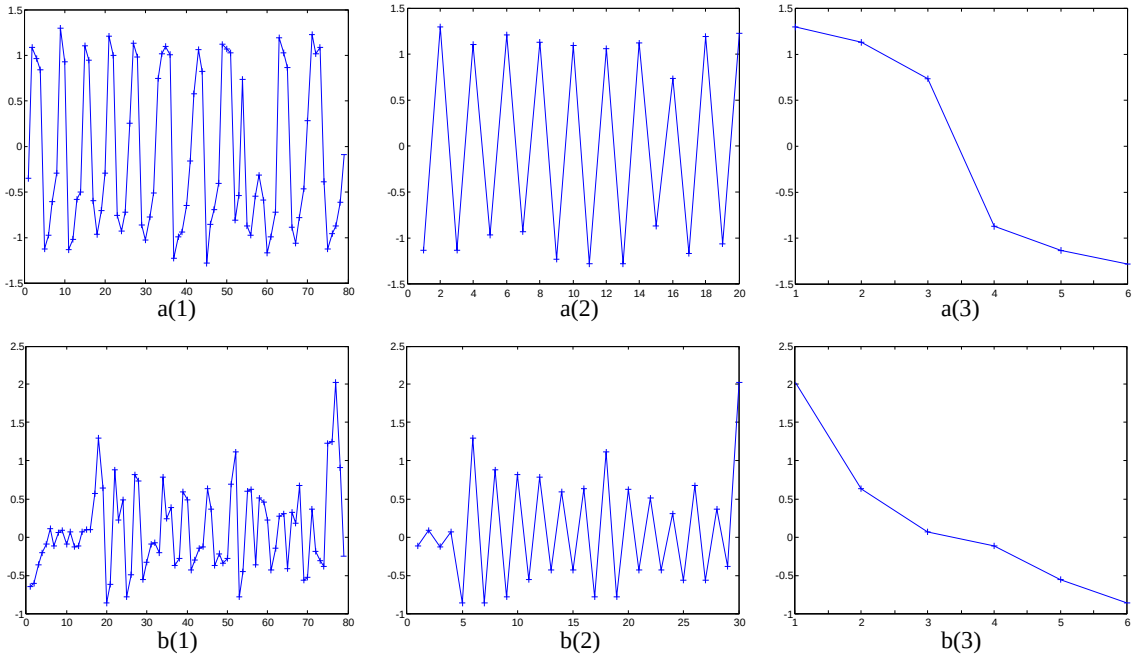

Figure 3. Feature extraction from optical values. The horizontal axis shows sequence number of time points, the vertical axis shows optical flow values based on two slices of two adjacent time points. a(1), a(2), and a(3) represent the original optical flow curve, local extrema curve, and feature values curve, respectively, of a normal signal. b(1), b(2), and b(3) correspond to similar curves, respectively, of an abnormal signal.

vector for each sagittal location, and is used as a basis for judging if a specific time series signal $v(t)$ associated with a sagittal location is normal or abnormal. Figure 3 a(3) and b(3) show the feature values (vertical axis) of the six features (horizontal axis) for the normal and abnormal samples in Figure 3 a(2) and b(2), respectively.

Data expansion by simulation

Since we had only 42 abnormal samples in our data sets of total sample size 380, we created additional abnormal samples by simulation starting from normal samples which were sufficient in number. For simulation, we took random time points in the normal samples and reduced or increased their flow values to one-third of the original value. In this manner, we created 118 additional abnormal samples from normal samples and utilized 160 samples each for the normal and abnormal classes for our machine learning strategy.

Model training

We employed a support vector machine (SVM) classifier to detect abnormal samples. The classification principle of SVM

is to find an optimal hyperplane as a decision surface under a linear separability condition, such that the decision surface will maximize the margin between positive and negative examples, thus minimizing classification error [5]. Choosing the parameters of the SVM classifier properly is important for establishing a model of identification of abnormal breathing signals [7]. An SVM model that automatically adjusts the parameters is used to train the classifier. In the model training process, abnormal samples are used as positive samples, and normal samples are used as negative samples. Our goal of model training is to reduce false negatives (FNs) as much as possible to avoid calling abnormal signals normal. In other words, we weigh reduction of FNs more heavily than that of false positives (FPs) to avoid calling normal signals abnormal. (The reason for this strategy is that, if we can achieve 0 FN rate, then even at the cost of losing some normal signals, we can be confident that there are no abnormal signals present in our data which would obviate the need for manually checking the data sets for abnormal signals.) We achieve this by stepping through two parameters of SVM within a certain range: penalty coefficient C of the cost function and kernel function parameter g of the radial basis function.

3. EXPERIMENTS AND RESULTS

A test dataset of 80 samples containing 40 positive samples and 40 negative samples is used to test our classification model, and the remaining 80 (40 positive and 40 negative) were used to train the model. Table 1 shows the results of 10 repeated experiments where different sets of data were selected for training and testing. In our experiments, we randomly selected a part of the real data and a part of the simulation data. In Table 1, FN and FP rates represent the rate of calling abnormal signals normal and calling normal signals abnormal, respectively. "Acc" represents the classification accuracy for test data. "Num_Real" represents the number of real abnormal samples randomly selected in each experiment. "Acc_Real" represents the classification accuracy of real abnormal data.

In our 10 experiments, the average FN rate and FP rate reached 5% and 26%, respectively. The accuracy over all (real and simulated) samples was 85%. The optimized set up of the classification model is such that it weakens the discriminating ability of normal data. In all real samples, 82% of the abnormal data were screened out. This accuracy is lower than for the mixed test dataset and is expected to be more accurate and closer to the latter after obtaining more real data in the future.

Table 1. The results of 10 experiments

No	FP Rate	FN Rate	Acc	Num_Real	Acc_Real
1	0.05	0.00	0.98	5	1.00
2	0.20	0.08	0.86	12	0.75
3	0.15	0.13	0.86	10	0.50
4	0.28	0.00	0.86	**7**	1.00
5	0.38	0.03	0.80	10	0.90
6	0.38	0.05	0.79	9	0.78
7	0.28	0.03	0.85	10	0.90
8	0.43	0.08	0.75	9	0.67
9	0.33	0.03	0.83	8	0.88
10	0.13	0.10	0.89	10	0.80
Mean	0.26	0.05	0.85	9	0.82

4. CONCLUSIONS

The study of TIS to establish biomarkers for the underlying pathophysiology and patient treatment outcomes is very important. Currently, this area is lacking such knowledge and investigations. Highly automated data analysis of thoracic dMRI data sets from patients with TIS aims at discovering such scientifically well-established biomarkers. This paper proposes a method to handle one issue related to automated processing of such dMRI data sets for this clinical application. While free-breathing acquisitions are natural and unencumbering to patients, they pose some technical challenges due to the natural breathing behavior of often very sick TIS patients. In this paper, to detect abnormal breathing patterns in free-breathing thoracic dMRI acquisitions, we devised an optical-flow-based technique to generate "respiratory signals" and a machine learning technique to distinguish between normal signals and abnormal signals. Our goal was to reduce as much

as possible (ideally to zero) the FNs in detecting truly abnormal signals. We achieved ~5% FN rate although the FP rate was higher at ~25%. A higher FP rate is acceptable for our goal as explained above at the cost of discarding some normal signals as abnormal whereas truly abnormal signals are excluded most (ideally 100%) of the time for our 4D construction method [1]. The method may be useful in other pediatric and non-pediatric clinical applications involving dynamic thoracic imaging.

ACKNOWLEDGEMENT

This research is partly supported by a Frontier grant from the Children's Hospital of Philadelphia. The training of Mr. Changjian Sun in the Medical Image Processing Group, Department of Radiology, University of Pennsylvania, Philadelphia, for the duration of two years is supported by the China Scholarship Council.

REFERENCES

[1] Tong, Y., Udupa, J. K., Ciesielski, K. C., Wu, C., McDonough, J. M., & Mong, D. A., et al. (2017). Retrospective 4D MR image construction from free-breathing slice acquisitions: a novel graph-based approach. Medical Image Analysis, 35, 345-359.

[2] Campbell RM Jr, M. D., Mayes, T. C., Mangos, J. A., Willey-Courand, D. B., & Kose, N., et al. (2003). The characteristics of thoracic insufficiency syndrome associated with fused ribs and congenital scoliosis. Journal of Bone & Joint Surgery American Volume, 85-A(3), 399.

[3] Campbell RM Jr, & Smith MD. (2007). Thoracic insufficiency syndrome and exotic scoliosis. Journal of Bone and Joint Surgery-American Volume, 89 Suppl 1(suppl 1), 108.

[4] Barron, J. L., Fleet, D. J., & Beauchemin, S. S. (1992). Performance of optical flow techniques. Computer Vision and Pattern Recognition, 1992. Proceedings CVPR '92. 1992 IEEE Computer Society Conference on IEEE,12, 236-242.

[5] Cortes, C., & Vapnik, V. (1995). Support-vector networks. Machine Learning, 20(3), 273-297.

[6] Cai, J., Chang, Z., Wang, Z., Paul, S. W., & Yin, F. F. (2011). Four-dimensional magnetic resonance imaging (4d-MRI) using image-based respiratory surrogate: a feasibility study. Medical Physics, 38(12), 6384-6394.

[7] Aydin, I., Karakose, M., & Akin, E. (2011). A multi-objective artificial immune algorithm for parameter optimization in support vector machine. Applied Soft Computing, 11(1), 120-129.